UDC 621.313 https://doi.org/10.20998/2074-272X.2026.3.02

A. Dilmi, A. Bouzida, N. Yassa, B. Fares

# Analysis of the external network parameters influence on the operating characteristics of self-excited induction generators

***Introduction**. Self-excited induction generators (SEIGs) play a vital role in renewable energy systems, particularly in remote regions. However, their performance is highly sensitive to excitation capacitance, rotor speed and load variations, making stability and reliability key challenges. **Problem.** Simplified analytical models fail to capture the complex internal interactions within SEIGs, limiting the analysis of how external network variations influence their dynamics. Moreover, the gradual degradation of excitation capacitors, a common fault in practice, significantly reduces generator efficiency. The **goal** of this work is to analyze the influence of excitation capacitance, rotor speed and load variations on SEIG performance, focusing on gradual capacitor degradation and open-phase faults to provide guidelines for reliable and efficient design. **Methodology.** Finite element modeling (FEM) with ANSYS Maxwell is used to accurately simulate electromagnetic and mechanical dynamics under realistic operating conditions. **Results.** Simulations show how changes in capacitance, rotor speed and load greatly affect voltage and current stability. Capacitor faults and open-phase conditions cause current distortion, voltage unbalance and reduced efficiency. **Scientific novelty** of this work lies in the FEM-based analysis of gradual excitation capacitor degradation in SEIGs. It was determined that this degradation directly impacts voltage balance, current waveform distortion and overall efficiency. **Practical value.** The findings provide clear guidelines for selecting optimal excitation capacitance and load ranges, reducing costs while enhancing the reliability and efficiency of SEIGs, particularly in isolated regions. Also this study offers new physical insight and a reliable framework for generator condition monitoring and design optimization.* References 24, tables 1, figures 12.

*Key words:* **self-excited induction generator, voltage stability, current distortion, reliability enhancement, rotor, capacitor.**

***Вступ.** Автономні асинхронні генератори (SEIGs) відіграють життєво важливу роль у системах відновлюваної енергетики, особливо у віддалених регіонах. Проте їхня продуктивність високочутлива до ємності збудження, швидкості ротора та змін навантаження, що робить стабільність та надійність ключовими викликами. **Проблема.** Спрощені аналітичні моделі не здатні відобразити складні внутрішні взаємодії в SEIG, що обмежує аналіз того, як коливання зовнішньої мережі впливають на їхню динаміку. Крім того, поступова деградація конденсаторів збудження, що є поширеною несправністю на практиці, суттєво знижує ефективність генератора. **Метою** роботи є аналіз впливу ємності збудження, швидкості ротора та змін навантаження на продуктивність SEIG, зосереджуючись на поступовій деградації конденсаторів та обривах фаз, щоб надати рекомендації для надійного та ефективного проєктування. **Методологія.** Для точного моделювання електромагнітної та механічної динаміки в реалістичних робочих умовах використовується моделювання методом скінченних елементів (FEM) за допомогою програмного комплексу ANSYS Maxwell. **Результати.** Моделювання показує, як зміни ємності, швидкості ротора та навантаження значно впливають на стабільність напруги та струму. Несправності конденсаторів та умови обриву фази спричиняють спотворення струму, дисбаланс напруги та зниження ефективності. **Наукова новизна** роботи полягає в аналізі поступової деградації конденсаторів збудження в SEIG, заснованому на FEM. Встановлено, що ця деградація безпосередньо впливає на баланс напруги, спотворення форми хвилі струму та загальну ефективність. **Практична цінність.** Отримані результати надають чіткі рекомендації для вибору оптимальної ємності збудження та діапазонів навантаження, знижуючи витрати та одночасно підвищуючи надійність і ефективність SEIG, особливо у віддалених регіонах. Також це дослідження пропонує нове фізичне розуміння та надійну основу для моніторингу стану генератора та оптимізації його проєктування.* Бібл. 24, табл. 1, рис. 12.

*Ключові слова:* **асинхронний генератор з самозбудженням, стабільність напруги, спотворення струму, підвищення надійності, ротор, конденсатор.**

**Introduction.** With the increasing integration of wind energy into modern power systems, the demand for reliable and cost-effective standalone generation solutions has grown, particularly in isolated and rural regions [1].

Among the available options self-excited induction generators (SEIGs) have emerged as an attractive choice due to their simple construction, cost-effectiveness, and ability to operate without external excitation sources. SEIGs offer several advantages, including a robust design, low maintenance requirements, and the use of a brushless squirrel-cage rotor. Moreover, their nonlinear voltage speed characteristic, shaped by magnetic saturation, enables stable operation even under slight rotor speed variations beyond the rated value [2].

Despite these advantages, the practical deployment of SEIGs requires continuous performance assessment, as they are highly sensitive to excitation capacitance, rotor speed, and load variations [3]. Faults and parameter variations can significantly degrade SEIG performance. In particular, excitation capacitor failures or open-phase conditions disturb the excitation balance, leading to distorted stator currents, unstable torque, and voltage fluctuations, which may escalate into complete system breakdown [4]. While the minimum and maximum capacitance levels required for self-excitation are well known, selecting and maintaining optimal values under real operating conditions remains a technical challenge [5].

To overcome these limitations, this study adopts the finite element modeling (FEM) to model SEIGs with high accuracy under both healthy and faulty conditions. The machine is first simulated as a motor and then transitioned to generator mode once the rotor exceeds synchronous speed, with self-excitation sustained by a connected capacitor bank [6]. Variations in capacitance, rotor speed, and load are investigated systematically, along with the impact of capacitor disconnect and open-phase faults on generator dynamics.

The **goal** of this work is to analyze the influence of excitation capacitance, rotor speed and load variations on SEIG performance, focusing on gradual capacitor degradation and open-phase faults to provide guidelines for reliable and efficient design.

**Literature review.** Induction machines have been widely investigated for use as generators in isolated applications. In [7], the authors proposed and evaluated series compensation techniques to improve the high-power variable speed operation of SEIGs, showing enhanced stability and power quality, which strengthens the reliability and practical feasibility of these generators in modern energy systems. Meanwhile, in [8] authors focused on employing the dragonfly algorithm for transient and steady-state analysis of SEIGs, highlighting the potential of computational intelligence methods in performance modeling rather than direct operational enhancement. Furthermore, practical applications of these machines have been presented in [9].

SEIGs offers several advantages, including robustness, light weight, compact size, and a brushless structure that reduces maintenance requirements and losses, making it a cost-effective solution. Moreover, SEIGs are characterized by simple operation and fast dynamic response, which further enhance their suitability for small-scale power generation.

In [10] an experimental investigation was conducted to evaluate and compare the performance of a SEIG and a permanent magnet synchronous generator for standalone renewable energy applications. The study utilized a micro-hydro turbine to drive both generators and examined their behavior under different load scenarios, including resistive heating and an induction motor-driven pump. With a focus on maintaining constant voltage and frequency in isolated systems, the research aimed to identify a simple, cost-effective, and reliable solution without relying on power electronic switches for reactive power compensation. The findings highlighted the viability of SEIGs as an economical and practical option for small-scale independent power generation.

Several studies have addressed parameter identification, voltage regulation, and performance optimization under steady-state, transient, and dynamic operating conditions [11, 12]. Authors [13] proposed an improved DSTATCOM control scheme using an enhanced phase-locked loop based on the current synchronous detection method, resulting in better terminal voltage regulation and enhanced power quality. In addition, in [14] were analyzed open-circuit capacitor faults in SEIGs and demonstrated that such faults can reduce torque to zero, destabilizing the system. Their approach utilized the Hilbert-Huang transform for fault detection. However, this study did not consider capacitor aging. In contrast**,** our work addresses this gap by evaluating the effects of capacitor aging on SEIG performance and reliability. Furthermore, we expand the study to include variations in capacitor capacity, load changes, rotor speed fluctuations, and phase-opening faults, providing a comprehensive assessment of factors influencing SEIG operation.

However, most previous studies rely on traditional SEIG modeling approaches, such as small-signal or *d-q* axis models, which often fail to capture the nonlinear behavior accurately under variable operating conditions, such as variations in load, rotor speed, and capacitance. In comparison, the present study employs the FEM, a robust and reliable approach capable of accurately representing the magnetic field and dynamic behavior of the generator. This methodology enhances the credibility of the results and addresses the limitations found in prior research.

**Presentation of the main material.** The FEM analyzes magnetic fields by considering factors such as the geometry of the magnetic circuit, the arrangement of stator windings and rotor bars, the presence of slots around the air gap, and the nonlinear characteristics of ferromagnetic materials [15]. Moreover, the behavior of electromagnetic systems is fundamentally governed by Maxwell's equations, which describe the essential relationships between electric and magnetic fields, as well as the intrinsic properties of various materials. These equations form the foundation for modeling and analyzing electromagnetic phenomena. In this context, it is crucial to integrate motion with the field equations within the FEM [16–18] to ensure an accurate and comprehensive representation of the system's dynamic behavior.

The general 2D formulation of Maxwell's equations is expressed as:

$$\nabla\times\boldsymbol{E} = -\partial\boldsymbol{B}/\partial t. \qquad (1)$$

This equation describes how a time-varying magnetic field induces a circulating electric field, where $\boldsymbol{E}$ is the electric field intensity; $\boldsymbol{B}$ is the magnetic flux density; $t$ is time; $\nabla$ is the curl operator denoting the rotational derivative of a vector field.

The Maxwell–Ampere law is expressed as follows:

$$\nabla\times\boldsymbol{H} = \boldsymbol{J}_e + \partial\boldsymbol{D}/\partial t. \qquad (2)$$

where $\boldsymbol{H}$ is the magnetic field intensity; $\boldsymbol{J}_e$ is the conduction current density; $\boldsymbol{D}$ is the electric flux density. In practical applications, particularly at industrial frequencies, the displacement current term $\partial\boldsymbol{D}/\partial t$ is very small and can be neglected. Thus, (2) simplifies to:

$$\nabla\times\boldsymbol{H} = \boldsymbol{J}_e. \qquad (3)$$

The relationship between the electric flux density and the free electric charge density $\rho_e$ is given by:

$$\nabla\cdot\boldsymbol{D} = \rho_e. \qquad (4)$$

Since the divergence of the curl of any vector field is always zero, applying this property to the Maxwell–Ampere law leads to the general continuity equation:

$$\nabla\cdot(\nabla\times\boldsymbol{H}) = \nabla\cdot\boldsymbol{J}_e = 0. \qquad (5)$$

This equation represents the conservation of electric charge, implying that, in steady-state or low-frequency applications where the displacement current is negligible $\partial\boldsymbol{D}/\partial t \approx 0$ and charge accumulation is minimal $\partial\rho_e/\partial t \approx 0$, the net current entering a closed surface is equal to the net current leaving it.

The electromagnetic behavior of materials is governed by Ohm's law in differential form:

$$\boldsymbol{J}_e = \sigma\cdot\boldsymbol{E}, \qquad (6)$$

where $\sigma$ is the electrical conductivity of the material.

The electric flux density can be formulated as:

$$\boldsymbol{D} = \varepsilon\cdot\boldsymbol{E} = \varepsilon_0\cdot\varepsilon_r\cdot\boldsymbol{E}, \qquad (7)$$

where $\varepsilon_0$ is the vacuum permittivity; $\varepsilon_r$ is the relative permittivity.

The magnetic flux density can be written as:

$$\boldsymbol{B} = \mu\cdot\boldsymbol{H} = \mu_0\cdot\mu_r\cdot\boldsymbol{H}, \qquad (8)$$

where $\mu$ is the permeability; $\mu_0$ is the vacuum permeability; $\mu_r$ is the relative permeability.

In summary, these equations form the basis for modeling electromagnetic fields and, within the FEM, allow accurate simulation of complex systems under dynamic conditions. The accurate assessment of the minimal capacitance necessary for SEIG is of considerable practical significance. Numerous numerical approaches for determining the requisite excitation capacitance have been recorded in prior studies [19].

This work derived the precise values of the minimum capacitance required for self-excitation based on (9) [20]:

$$C_{\Delta\min} = Q_{gen} / 3U^2\omega, \quad (9)$$

where $C_{\Delta\min}$ is the minimum capacitance per phase in Δ connection; $Q_{gen}$ is the reactive power that must be supplied by the excitation capacitors to establish self-excitation in the generator; the angular frequency $\omega = 2\pi f$, where $f$ is the supply frequency; $U$ is the phase voltage.

Initially, the reactive power consumed by the asynchronous machine while operating as a motor $Q_{mot}$ is determined as:

$$Q_{mot} = (P_n/\eta_{mot})\cdot\tan(\cos^{-1}\varphi_{mot}), \quad (10)$$

where $P_n$ is the rated mechanical power; $\eta_{mot}$ is the efficiency of the driving mechanism; $\varphi_{mot}$ is the power factor angle during motor operation.

After evaluating the reactive power consumed in motor mode $Q_{mot}$, the corresponding reactive power in generator mode $Q_{gen}$ can be computed as:

$$Q_{gen} = (\sin\varphi_{gen} / \sin\varphi_{mot})\cdot Q_{mot}, \quad (11)$$

where $\varphi_{gen}$ is the power factor angle during generator operation [21].

This study presents a numerical analysis of a SEIG designed to operate with excitation capacitors of 151 μF. The detailed specifications of the SEIG are listed in Table 1.

Table 1

Parameters of the SEIG

| Parameter | Value | Parameter | Value |
|---|---|---|---|
| Rated power | 4 MW | Rotor slots | 52 |
| Rated voltage | 3000 V | Bs0 rotor slot | 3.5 mm |
| Coupling method | Wye | Bs1 rotor slot | 13 mm |
| Number of poles | 2 | Bs2 rotor slot | 13 mm |
| Rated speed | 3135 rpm | Hs0 rotor slot | 4.3 mm |
| Operating temperature | 75° | Hs01 rotor slot | 2.7 mm |
| Stator slots | 54 | Hs1 rotor slot | 4.85 mm |
| Hs0 stator slot | 4.5 mm | Hs2 rotor slot | 40.25 mm |
| Hs2 stator slot | 115mm | Hs1 stator slot | 2.4 mm |
| BS2 stator slot | 18.2 mm | Bs1 stator slot | 21.16 mm |

**Geometry and regions.** Modeling half or a quarter of the machine is possible due to symmetry; however, once asymmetries are introduced, a full machine model is required to accurately capture the physical phenomena.

The modeling procedure begins with the definition of the stator slot geometry (Fig. 1), where the slot dimensions and winding layout are carefully specified to reflect the real machine design. The rotor slots were designed with a slight skew angle to reduce cogging torque and mitigate magnetic locking between the stator and rotor teeth.

Next, the rotor slot geometry is constructed, as shown in Fig. 2. Ensuring that the bar placement and end-ring connections are properly represented.

The stator and rotor of the studied generator were designed and modeled within the Ansys Maxwell simulation environment. Figure 3 shows the geometric configuration of the notch structure along with the distribution of slots and their corresponding parameters.

The meshing process is a fundamental step in numerical simulation, as the quality and density of the mesh directly affect the accuracy and reliability of the results. A finer mesh is typically applied to critical regions such as slots, the air gap, and areas with sharp variations in electric and magnetic fields, where abrupt field changes may cause significant errors if not accurately resolved.

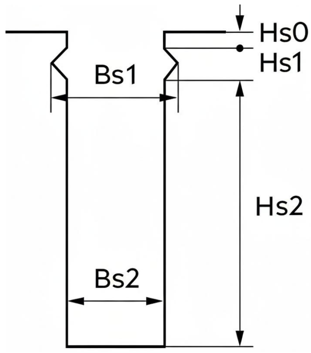


Fig. 1. Stator slot

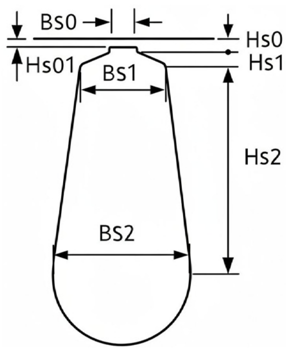


Fig. 2. Rotor slot

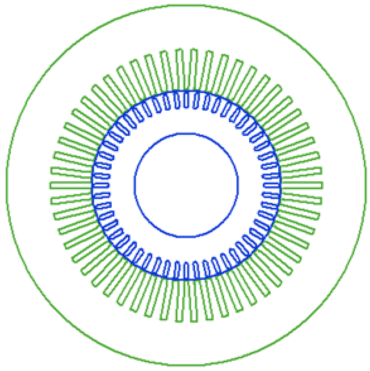

Fig. 3. Geometry of stator and rotor

Conversely, larger and coarser elements are utilized in regions where the fields vary gradually, reducing the computational load and enhancing simulation efficiency. Moreover, the choice of element type – whether triangular, quadrilateral, or higher-order elements – significantly influences both solution accuracy and computational speed. These strategies collectively aim to achieve an optimal balance between precision and computational efficiency in the analysis of electrical generators. The geometry, mesh and phases distribution of the studied model are shown in Fig.4.

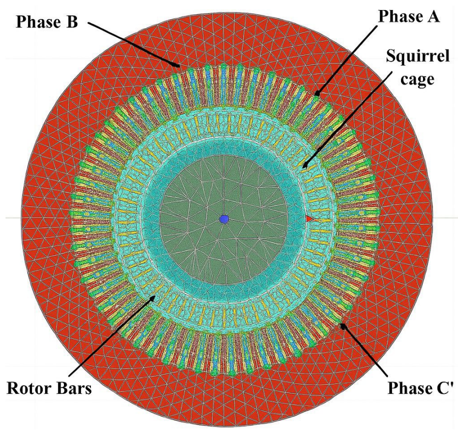


Fig. 4. The geometry, mesh and phases distribution of the studied model

In the final stage, the 2D model is created, with all the required parameters, boundary conditions and phase and winding distributions accurately represented. The magnetic field distribution is depicted, providing a detailed map of flux lines and field density, which allows for an in-depth analysis of the machine's electromagnetic performance. Figure 5 shows the Maxwell 2D model and the corresponding magnetic field distribution.

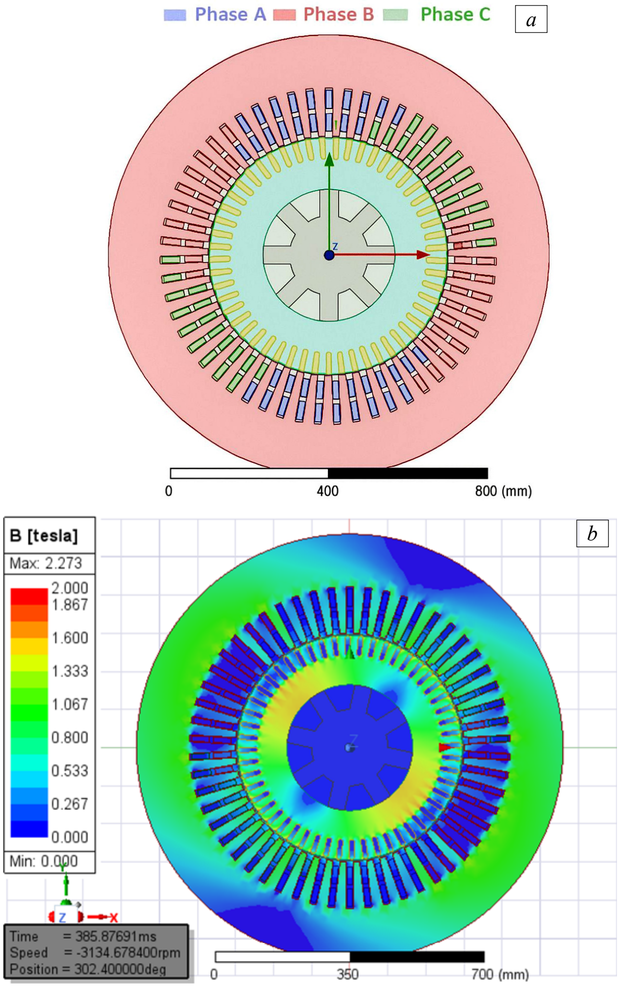

Fig. 5. Maxwell 2D model (*a*) and the distribution of magnetic flux density (*b*)

This sequential workflow from geometry definition, through meshing, to field distribution ensures a reliable finite element representation of the machine, forming the foundation for accurate simulations and further performance evaluation.

**Simulation results and discussion.** The developed model is tested using the time stepping FEM to evaluate its performance under no-load conditions. The voltage output of the SEIG remains stable at 3 kV, while the stator current settles at 550 A without distortions, confirming that the generator operates reliably in this state.

Figure 6 shows the root mean square (RMS) values of both voltage and current, clearly illustrating their stable and distortion-free behavior.

**Influence of capacitance value.** In [22] a steady-state equivalent circuit model of a 5 kW (SEIG) was employed, focusing on optimizing shunt and series capacitances for frequency regulation.

Two optimization techniques, the genetic algorithm (GA) and the gravitational search algorithm (GSA), were applied to determine the optimal capacitor values under resistive and resistive–inductive loads.

The results showed that optimized capacitor sizing significantly reduced frequency deviation and enhanced operational stability, with comparable performance between the two methods.

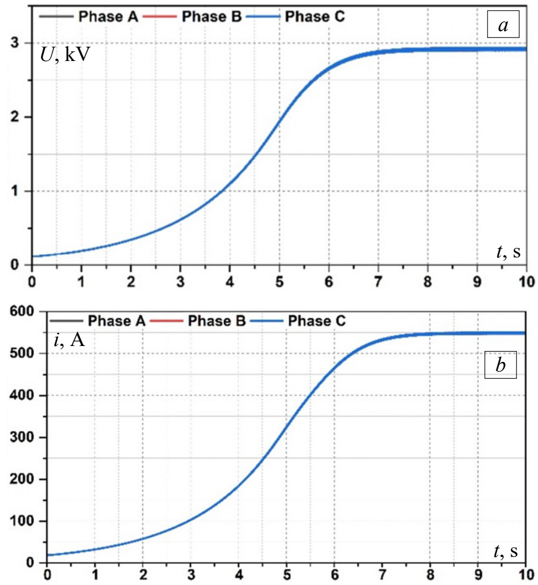

Fig .6. The RMS values of voltage (*a*) and current (*b*) under the no-load condition

Since that study focused on the effect of capacitance on frequency, our work emphasizes the impact of excitation capacitance on the self-excitation time, voltage, and current of the SEIG. Starting from the minimum capacitance of $C_{\Delta}$ = 452 μF, the value was progressively increased to 900 μF, 1200 μF and 1500 μF. The corresponding results are presented in Fig. 7, which shows the influence of excitation capacitance on the voltage build-up process of the generator. For a capacitance of 900 μF, the voltage stabilizes at approximately 3.6 kV after nearly 3 s, indicating slower excitation, with the corresponding RMS current reaching about 1.53 kA. Increasing the capacitance to 1200 μF raises the voltage to around 3.9 kV within 2 s, accompanied by a steady-state current of nearly 1.55 kA. At 1500 μF the generator achieves nearly 4.2 kV in less than 1.5 s, while the current rises to approximately 2.3 kA, highlighting a significant improvement in both excitation time and output magnitude.

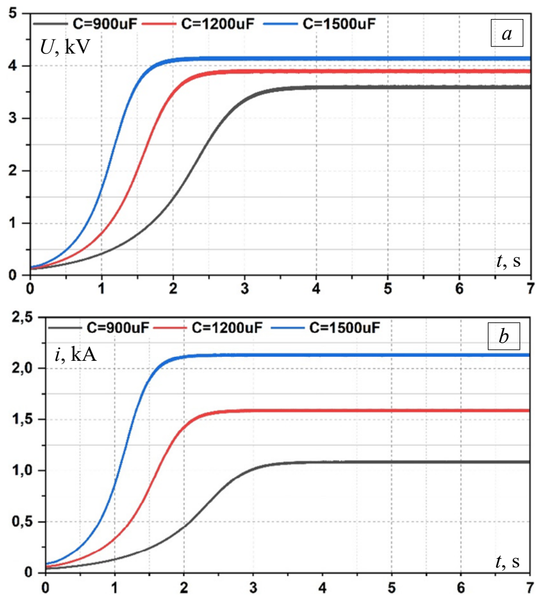

Fig. 7. RMS values of voltage (*a*) and current (*b*) under variable capacitor value

These results clearly demonstrate that higher capacitance values reduce the self-excitation time, but they also increase the voltage and current beyond the generator's capacity, which may put it at risk. This highlights the importance of careful and precise selection of the appropriate capacitor size.

Moreover, our experiments show that selecting a capacitance up to 10 % above the minimum required is beneficial, as it ensures self-excitation, improves voltage stability, and enhances the power factor. However, this should be regarded as a practical guideline based on the studied operating conditions, since the actual impact depends on the generator characteristics, rotational speed, and the connected load.

**Influence of speed.** The second parameter influencing the generator's electrical characteristics is rotor speed. We set the capacitance value at $C_{\Delta}$ = 900 µF and created a variable speed profile (Fig. 8).

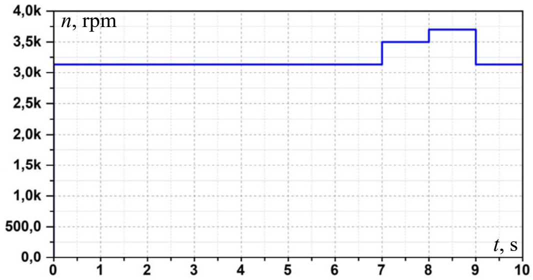


Fig. 8. Profile of variable rotor speed

Rotor speed fluctuations are a key factor influencing the electrical characteristics of the induction generator, as illustrated in Fig. 9.

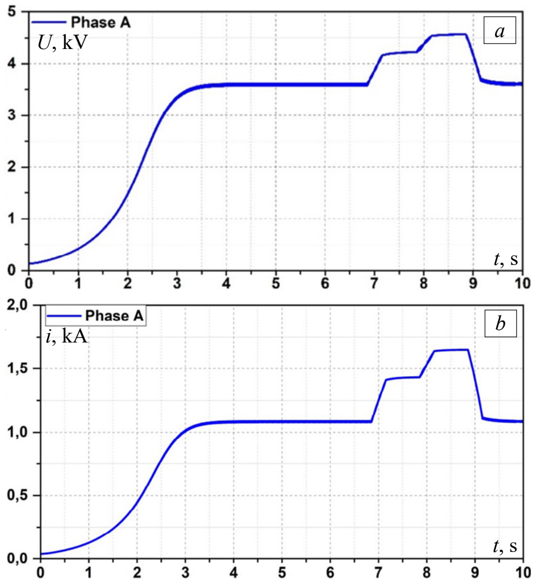


Fig. 9. RMS values of voltage (*a*) and current (*b*) under a variable rotor speed profile

An increase in speed leads to higher voltage and current, while a decrease reduces these values. The analysis results indicate that when the rotor speed increased by 25 rpm above the synchronous speed of 3110 rpm and stabilized at 3135 rpm, the start-up was smooth, as observed in the current and voltage signals during the period from 0 to 2.5 s. In contrast, when the rotor speed rose significantly above this value, the voltage exceeded 3 kV, pushing the generator beyond its design capacity, increasing its temperature, and potentially leading to failure. Accordingly, this study concludes that the rotor speed should not exceed 30 % above the synchronous speed (approximately 4043 rpm) in order to avoid operational risks and ensure the stability and safety of the generator. To address this, control techniques such as blade angle adjustment in wind turbines or advanced electronic systems for voltage and current regulation are employed to maintain safe operation. The ability of the induction generator to withstand such fluctuations without voltage collapse is essential for grid stability and for enhancing energy production efficiency.

**Influence of load**. This section investigates the impact of load variation on the generator's performance. The study in [23] analyzed and simulated wind-driven SEIG supplying isolated DC loads using a MATLAB/Simulink model, focusing solely on DC loads without considering AC or variable loads more comprehensively. In contrast, in our study, a balanced 3-phase load of 3 Ω is applied at $t$ = 0.05 s after the generator reaches steady-state, followed by successive tests with loads of 5 Ω and 10 Ω. The resulting voltage and current responses, shown in Fig. 10, highlight the nonlinear behavior of the SEIG under varying load conditions. For a 10 Ω load, the generator maintains a nearly constant voltage of 2.8–2.9 kV with a steady current of 0.55–0.6 kA, demonstrating stable operation.

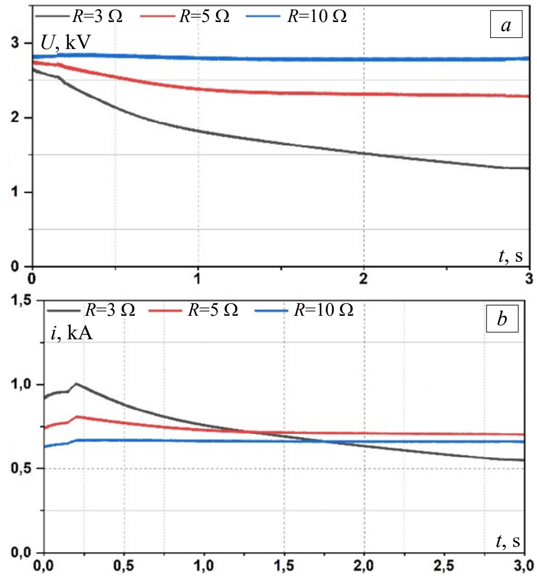


Fig. 10. The RMS values of voltage (*a*) and current (*b*) under different load values

At 5 Ω, the voltage gradually decreases to around 1.4–1.5 kV, while the current stabilizes at approximately 0.8 kA. In contrast, a 3 Ω load leads to a pronounced decline in voltage, falling from ~2.6 kV to ~1.4 kV, accompanied by a current drop from ~1.2 kA to ~0.55 kA. These results demonstrate that heavier loads significantly accelerate voltage decay while only moderately affecting the current, emphasizing the importance of load management to preserve generator stability and efficiency.

**Influence of open phase fault**. Previous research in [14] investigated the performance of SEIG under phase fault conditions. The study focused on a line–line fault between phases A and B. During this fault, the voltage of the directly affected phase A dropped immediately to zero at $t$ = 1.6 s, while the voltages of the remaining healthy phases B and C decreased shortly afterward at $t$ = 1.68 s. At the same time, a sudden surge in current occurred in the affected lines during the initial cycles following the fault.

However, this study did not explicitly examine the effects of an open-phase fault, in which a single phase is suddenly disconnected from the supply.

In the present study, phase A was intentionally interrupted at $t$ = 7 s after the generator reached steady-state operation under load, as shown in Fig. 11. This disconnection caused the current in the faulty phase to collapse to zero, while the currents in the remaining phases decreased, forcing the generator to operate in a single-phase mode. The faulty phase also exhibited a transient voltage rise before stabilizing at a lower value, resulting in a clear imbalance among the 3-phase voltages. These disturbances can compromise the stability of control and protection systems, as voltage and current fluctuations may trigger protective relays and disconnect the generator from the network, potentially causing unplanned outages and economic losses. The findings emphasize the necessity of advanced monitoring and protection strategies, including vibration analysis, thermal imaging, and real-time diagnostics supported by predictive algorithms, to enable early fault detection and corrective actions before severe damage occurs.

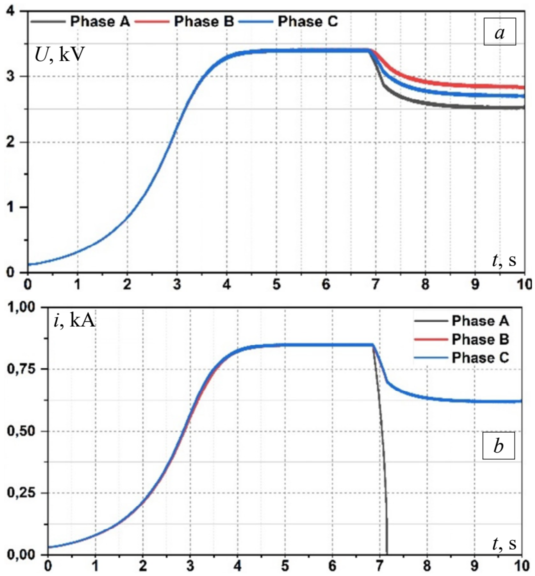

Fig. 11. RMS values of voltage ($a$) and current ($b$) under an open phase A condition

**Influence of capacitor degradation.** The progressive reduction in the capacitance of the excitation capacitor due to aging, thermal, or electrical stress [24] is a common fault in SEIGs, directly affecting their electrical stability. Figure 12 illustrates the current and voltage waveforms during this fault.

The gradual capacitor failure occurs while the generator is in operation, between 5 s and 7 s, leading to a drop in current from approximately 480 A to 370 A, followed by voltage waveform distortion. This gradual degradation reduces efficiency and shortens the generator's service life. Unlike previous studies that mainly focused on sudden disconnection, this work provides a precise analysis of the mechanism of gradual capacitance collapse using FEM, enabling researchers and engineers to gain deeper insights and enrich the understanding of generator stability.

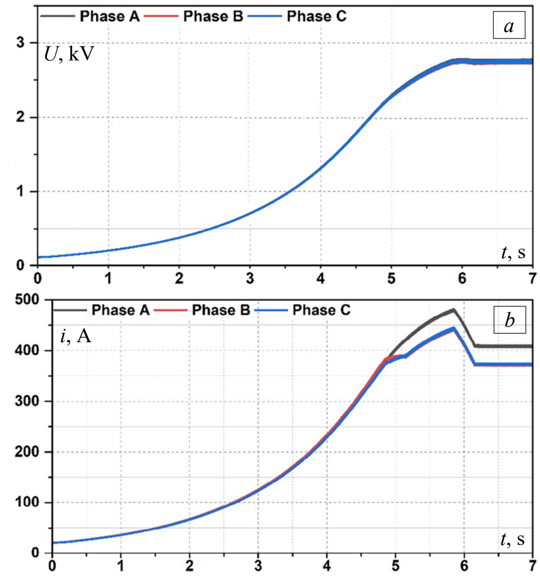

Fig. 12. RMS values of voltage ($a$) and current ($b$) under the condition of capacitor degradation

**Conclusions.** The main findings of this study are summarized through the analysis of internal and external factors influencing SEIG performance.

It was demonstrated that the excitation capacitance directly affects voltage stability and excitation time, as higher capacitance accelerates voltage build-up but increases the risk of overvoltage.

Regarding mechanical factors, rotor speed variation significantly influences voltage and current magnitudes, with stable operation ensured when the speed does not exceed 30 % above the synchronous value. Under external conditions, load variations revealed the nonlinear behavior of SEIGs, where heavier loads accelerate voltage decay, emphasizing the importance of proper load management.

Furthermore, open-phase faults cause severe voltage imbalance and current distortion, highlighting the necessity of advanced protection mechanisms. Notably, the gradual degradation of excitation capacitors due to aging serves as a reliable fault indicator, as it reduces current amplitude and distorts voltage waveforms.

The FEM-based analysis proved to be an effective approach for evaluating generator stability under both healthy and faulty conditions. Based on these findings, it is recommended to maintain the excitation capacitance slightly above the minimum required value (by approximately 10 %) to ensure reliable self-excitation and improve the power factor.

**Conflict of interest**. The authors declare that they have no conflicts of interest.

REFERENCES

***1.*** Hafaiedh H., Saoudi Y., Benamor A., Chrifi–Alaoui L. Wind farms integration into power system with improved location and stability problem solving. *Electrical Engineering & Electromechanics*, 2025, no. 5, pp. 10-16. doi: https://doi.org/10.20998/2074-272X.2025.5.02.

***2.*** Belynda F., Abdelli R., Bouzida A. Stator current signal crossing for fault diagnosis of self-excited induction generators.

*Acta Polytechnica*, 2023, vol. 64, no. 5, pp. 293-304. doi: https://doi.org/10.14311/AP.2023.63.0293.
**3.** Shailly D., Chittora P., Singh M. Performance analysis of multiple delayed signal cancellation (MDSC) for power quality improvement for fixed speed SEIG-based distributed generation. *Electrical Engineering*, 2025, vol. 107, no. 8, pp. 10911-10930. doi: https://doi.org/10.1007/s00202-025-03068-w.
**4.** Kouchih D., Hachelaf R. Discrimination of Stator Asymmetries and Magnetic Saturation in Self-Excited Induction Generators. *Russian Electrical Engineering*, 2024, vol. 95, no. 5, pp. 417-424. doi: https://doi.org/10.3103/S1068371224700469.
**5.** Khan M.F., Khan M.R., Iqbal A. Effects of induction machine parameters on its performance as a standalone self excited induction generator. *Energy Reports*, 2022, vol. 8, pp. 2302-2313. doi: https://doi.org/10.1016/j.egyr.2022.01.023.
**6.** Catelas J.M.R., Fernandes J.F.P., Pérez-Sánchez M., López-Jiménez P.A., Ramos H.M., Branco P.J.C. Energy Efficiency and Stability of Micro-Hydropower PAT-SEIG Systems for DC Off-Grids. *Energies*, 2024, vol. 17, no. 6, art. no. 1382. doi: https://doi.org/10.3390/en17061382.
**7.** Ahmed M.M., Hassanein W.S., Enany M.A. Proposing and Evaluation of SC Techniques for Variable Speed High-Power Operation of SEIG. *IEEE Access*, 2020, vol. 8, pp. 20666-20675. doi: https://doi.org/10.1109/ACCESS.2020.2968976.
**8.** Singh G., Singh V.R. SEIG-based transient- and steady-state analysis using dragon fly approach. *Soft Computing*, 2023, vol. 27, no. 6, pp. 2993-3005. doi: https://doi.org/10.1007/s00500-022-07458-1.
**9.** Rajak M.K., Samanta J., Pudur R. A hardware-based novel approach for parallel operation of two differently rated SEIGs. *Results in Engineering*, 2023, vol. 17, art. no. 100825. doi: https://doi.org/10.1016/j.rineng.2022.100825.
**10.** Murali Krishna V.B., Sandeep V., Murthy S.S., Yadlapati K. Experimental investigation on performance comparison of self excited induction generator and permanent magnet synchronous generator for small scale renewable energy applications. *Renewable Energy*, 2022, vol. 195, pp. 431-441. doi: https://doi.org/10.1016/j.renene.2022.06.051.
**11.** Dewangan S., Vadhera S. Performance Evaluation of Multilevel Inverter in Variable Speed SEIG-Based Wind Energy System. *Arabian Journal for Science and Engineering*, 2022, vol. 47, no. 3, pp. 3311-3324. doi: https://doi.org/10.1007/s13369-021-06197-z.
**12.** Chanu L.K., Chakraborty S., Pudur R. Real-time analysis of voltage and frequency regulation of self-excited induction generator based micro hydro plant using generalized impedance controller. *Measurement: Sensors*, 2024, vol. 33, art. no. 101235. doi: https://doi.org/10.1016/j.measen.2024.101235.
**13.** Özer A.S., Sevilmiş F., Karaca H., Arabacı H. Enhanced control method for voltage regulation of DSTATCOM based SEIG. *Energy Reports*, 2022, vol. 8, pp. 839-847. doi: https://doi.org/10.1016/j.egyr.2022.05.191.
**14.** Dalei J., Mohanty K.B. Fault classification in SEIG system using Hilbert-Huang transform and least square support vector machine. *International Journal of Electrical Power & Energy Systems*, 2016, vol. 76, pp. 11-22. doi: https://doi.org/10.1016/j.ijepes.2015.09.009.
**15.** Patel A.N., Doshi P.J., Mahagoakar S.C., Panchal T.H. Optimization of cogging torque in interior permanent magnet synchronous motor using optimum magnet v-angle. *Electrical Engineering & Electromechanics*, 2023, no. 6, pp. 16-20. doi: https://doi.org/10.20998/2074-272X.2023.6.03.
**16.** Panchal T.H., Patel A.N., Patel R.M. Reduction of cogging torque of radial flux permanent magnet brushless DC motor by magnet shifting technique. *Electrical Engineering & Electromechanics*, 2022, no. 3, pp. 15-20. doi: https://doi.org/10.20998/2074-272X.2022.3.03.
**17.** Iegorov O.B., Kundenko M.P., Iegorova O.Y., Mardziavko V.A., Rudenko A.Y. The influence of the design of the stator winding of a synchronous-reactive generator on increasing its energy efficiency. *Electrical Engineering & Electromechanics*, 2025, no. 5, pp. 3-9. doi: https://doi.org/10.20998/2074-272X.2025.5.01.
**18.** Grechko O.M. Influence of the poles shape of DC electromagnetic actuator on its thrust characteristic. *Technical Electrodynamics*, 2024, no. 1, pp. 38-45. doi: https://doi.org/10.15407/techned2024.01.038.
**19.** Arya S.R., Maurya R., Giri A.K., Qureshi A., Baladhanautham C.B. Power quality solutions for effective utilization of single-phase induction generator using voltage source converter. *Energy Sources, Part A: Recovery, Utilization, and Environmental Effects*, 2025, vol. 47, no. 2, art. no. 1772414. doi: https://doi.org/10.1080/15567036.2020.1772414.
**20.** Samanta J., Chakraborty S., Sangno R., Pudur R. Study of power quality issues in a renewable-driven self-excited induction generator due to different loads at edge-off grid system. *E-Prime - Advances in Electrical Engineering, Electronics and Energy*, 2025, no. 11, art. no. 100885. doi: https://doi.org/10.1016/j.prime.2024.100885.
**21.** Abd el-Ghany H.A., Ahmed E.S., ELGebaly A.E. A Reliable Loss of Excitation Protection Technique Based on EPFA for Synchronous Generators. *IEEE Transactions on Power Delivery*, 2022, vol. 37, no. 3, pp. 1445-1455. doi: https://doi.org/10.1109/TPWRD.2021.3087538.
**22.** Paliwal S., Sinha S.K., Chauhan Y.K. Frequency Control of 5 kW Self-excited Induction Generator Using Gravitational Search Algorithm and Genetic Algorithm. *AI and IOT in Renewable Energy*, 2021, pp. 75-88. doi: https://doi.org/10.1007/978-981-16-1011-0_8.
**23.** Sakkoury K.S., Emara S., Ahmed M.K. Analysis of wind driven self-excited induction generator supplying isolated DC loads. *Journal of Electrical Systems and Information Technology*, 2017, vol. 4, no. 1, pp. 257-268. doi: https://doi.org/10.1016/j.jesit.2016.08.003.
**24.** Guan B., Zhen X. Noninvasive Online Capacitor Monitoring Method for Three-Level Converter Based on Active Neutral-Point Current Adjustment. *IEEE Transactions on Industrial Electronics*, 2024, vol. 71, no. 5, pp. 4320-4329. doi: https://doi.org/10.1109/TIE.2023.3283714.

*Received 02.10.2025*
*Accepted 22.12.2025*
*Published 02.05.2026*

*A. Dilmi*[1]*, PhD Student,*
*A. Bouzida*[1]*, PhD, Full Professor,*
*N. Yassa*[1]*, PhD, Associate Professor,*
*B. Fares*[2]*, PhD, Assistant Lecturer,*
[1] Materials, and Sustainable Development Laboratory (LMDD), Faculty of Applied Sciences, University of Bouira, Algeria,
e-mail: ali.dilmi@univ-bouira.dz (Corresponding Author).
[2] Industrial and Information Technology Laboratory (IITL), University of Bejaia, Algeria.

*How to cite this article:*
Dilmi A., Bouzida A., Yassa N., Fares B. Analysis of the external network parameters influence on the operating characteristics of self-excited induction generators. *Electrical Engineering & Electromechanics*, 2026, no. 3, pp. 11-17. doi: https://doi.org/10.20998/2074-272X.2026.3.02